Climatic Change (2010) 98:359–377
DOI 10.1007/s10584-009-9735-7

Potential changes in extremes and links with the Southern Annular Mode as simulated by a multi-model ensemble

Claudio G. Menéndez · Andrea F. Carril

Received: 23 June 2008 / Accepted: 3 August 2009 / Published online: 16 October 2009

Abstract We assess the likely changes in climate extremes under enhanced greenhouse gases over the southern extratropics, with emphasis in southern South America and sub-Antarctic seas, through the analysis of extreme indices measured from models participating in the IPCC 4th Assessment Report. We discuss how the anthropogenic climate change under A1B scenario influences both the patterns of mean change of extreme indices and the likelihood of occurrence of severe extreme indices. The likelihood of occurrence of a year with a large number of days with "warm" minimum temperatures is estimated to increase by a factor of 4 by the end of this century over most of the southern extratropics. By that time, the risk of "severe" precipitation intensity is projected to rise in most areas with the exception of the subtropical anticyclones, which experience particularly strong drying. Over the Southern Ocean this likelihood has increased to over 60%. Corresponding estimates of the changing likelihood for very long dry spells show a banded structure with positive ratios to the north of about 50° S and negative ratios in the sub Antarctic seas. In southern South America this risk about doubled between present and future climates. Then, we explore if the Southern Annular Mode influences the occurrence of severe extreme indices during the period 2070–2099. Its positive phase inhibits the extremely warm minimum temperatures in the Southern Ocean, with the exception of the eastern Bellingshausen Sea, and favors severe frost days to the north of

C. G. Menéndez (✉) · A. F. Carril
Centro de Investigaciones del Mar y la Atmósfera, CONICET/UBA,
Pabellon 2, Piso 2, Ciudad Universitaria, 1428 Buenos Aires, Argentina
e-mail: menendez@cima.fcen.uba.ar

C. G. Menéndez
Departamento de Ciencias de la Atmósfera y los Océanos,
Universidad de Buenos Aires, Buenos Aires, Argentina

the Ross Sea. Temperature indices show very little change induced by the SAM to the north of 50° S. Severe dry spells are inhibited during the positive phase along the sub Antarctic seas, while the mid-latitudes, including most of Patagonia, show the opposite behaviour. The Southern Ocean reveals a non-uniform distribution with both increases and decreases in the occurrence of heavier precipitation during positive SAM.

1 Introduction

Single extreme events cannot be attributed to anthropogenic forcing, as there is always a finite chance the event in question might have occurred naturally. However, the recent occurrence of different kinds of extremes throughout southern South America was accompanied by a general sense of societal concern that such phenomena were attributable in some measure to anthropogenic climate change. In order to deal with such concerns, we attempt to answer the question: how does anthropogenic climate change influence the likelihood of occurrence of severe weather phenomena? Our analysis will emphasize southern South America and the Southern Ocean.

For this reason, we use the indices related with daily temperature and precipitation extremes defined by Frich et al. (2002). These "extreme indices" (annual indicators derived from daily temperature and precipitation time series) were computed by some modeling centers from climate change simulations in the framework of the Fourth Assessment Report of the International Panel on Climate Change (IPCC AR4). Meehl et al. (2005) and Tebaldi et al. (2006) provide a first overview of projected changes in climate extremes from the IPCC AR4 model ensemble using Frich et al.'s indices. They analyze the trends in globally averaged values of extreme indices and the global spatial patterns of changes under different emissions rates. In these studies, the indices were only considered over continental areas. Kharin et al. (2007) also examine temperature and precipitation extremes and their potential future changes as simulated by the IPCC AR4 models, but they defined extremes in terms of 20-year return values of annual extremes.

In particular, the ability of the latest state-of-the-art climate models to simulate temperature and precipitation extremes was documented by Tebaldi et al. (2006) and Kharin et al. (2007) for the IPCC AR4 models. Other studies such as Meehl et al. (2007), Sillmann and Roekner (2008) and Alexander and Arblaster (2008) have compared indices for climate extremes from climate model simulations with observed data over different regions or continents. Overall, climate models simulate present-day warm extremes reasonably well on the global scale, as compared to estimates from reanalyses and observations (e.g., Kiktev et al. 2003, 2007; Christidis et al. 2005). Trends for the twentieth century generally agree with previous observational studies, providing a basic sense of reliability for the coupled models. The models' discrepancies in simulating cold extremes are generally larger than those for warm extremes, especially in sea ice-covered areas. Simulated present-day precipitation extremes are plausible in the extratropics, but uncertainties in extreme precipitation in the tropics are very large, both in models and available observationally based datasets (Kharin et al. 2007).

In the CLARIS region, Rusticucci et al. (2006) have concentrated on the comparison of Frich et al.'s indices based on observational data from 90 weather stations in South America with results from the IPCC AR4 models. This comparison shows that the models ensemble are able to realistically capture the observed climatological broad-scale patterns of temperature and precipitation indices, particularly in southeastern South America, although the quality of the simulations depends on the index, model and region under consideration. Rusticucci et al. (2009) further assess the simulation of extreme indices for this region.

To further explore the relationship between the changes in extremes and the extratropical circulation under changed climate, we attempt to answer a second question: to what degree can we relate the changes in extremes to changes in the Southern Annular Mode (SAM)? In particular, our aim is to assess if the climate extremes indices provided by the AR4 coupled models over the Southern Ocean and embedded land masses are sensitive to the phases of the SAM.

The SAM (Thompson and Wallace 2000) is characterized by a meridional seesaw in atmospheric mass between Antarctica and the mid-latitudes accompanied by an out-of phase relation in the strength of the zonal flow along 55–60° S and 35–40° S. When pressures are below (above) average over Antarctica and westerly winds are enhanced (reduced) over the Southern Ocean, the SAM is said to be in its high (low) index or positive (negative) phase. Transient climate simulations in general exhibit a trend in the SAM towards its positive phase with a strengthening of the circumpolar vortex and intensification of the circumpolar westerlies (e.g. Kushner et al. 2001; Cai et al. 2003; Rauthe et al. 2004; see also Section 9.5.3.3 in Hegerl et al. 2007). In general, models simulate a clear SAM but the shape and orientation of the spatial patterns display relatively large intermodel variations (Raphael and Holland 2006). According to the recent IPCC AR4, the spatial structure of the SAM is well captured by the ensemble of AR4 models but the realistic simulation of its amplitude and temporal variability is difficult to assess (see Section 8.4.1 in Randall et al. 2007). This characteristic is also present in atmospheric forced simulations (e.g. Carril and Navarra 2001). The pattern of observed temperature trends around Antarctica (warming over the Antarctic Peninsula and little change over the rest of the continent) is consistent with circulation changes associated with the trend in the SAM in the last half of the twentieth century (Thompson and Wallace 2000; Schneider et al. 2004). The composite of the IPCC AR4 models qualitatively captures the observed enhanced warming trend over the Antarctic Peninsula (Chapman and Walsh 2006).

The relationship between the SAM and surface features of the mean climate over the Southern Ocean and Antarctic Peninsula, through the analysis of simulations from a multimodel ensemble in the framework of the IPCC AR4, was documented in Carril et al. (2005) and Menéndez and Carril (2005). The SAM influences the extratropical climate, not only over the Southern Ocean and Antarctica, but over the southern continental regions as well, probably because changes in the SAM are linked with shifts in the location of the southern hemisphere (SH) storms (e.g. Pezza et al. 2007). The regional influence of the SAM on the mean climate has been documented in southern South America (Silvestri and Vera 2003; Haylock et al. 2006), western South Africa (Reason and Rouault 2005), and southern Australia (Meneghini et al. 2007; Hendon et al. 2007).

2 Key processes and methodology

2.1 Overview of physical mechanisms

According to the IPCC AR4 there are two dominant mechanisms that provide the conditions against which regionally specific factors operate in a global warming context: (1) an enhancement of the horizontal moisture fluxes in the atmosphere, and (2) a poleward shift in the extratropical wind and pressure fields (see Section 11.1.3 in Christensen et al. 2007). The first of these effects is a straightforward consequence of the increase in temperature and the resulting increase in atmospheric water vapor (e.g. Held and Soden 2006). The atmosphere is continually transporting water preferentially from some regions (such as the subtropical zones) to others (subpolar and equatorial zones). As this divergence/convergence is balanced by the difference between precipitation and evaporation, the pattern of precipitation minus evaporation will be enhanced. Even if the circulation does not change, wet regions get wetter and dry regions drier. The second effect is a poleward shift of the storm tracks and the accompanying general circulation, a robust response of the SH circulation to global warming across the IPCC AR4 models (Yin 2005; Christensen et al. 2007). The poleward shift of the midlatitude circulation is accompanied by a shift towards the high polarity of the SAM (e.g. Yin 2005; Hendon et al. 2007). While the SAM is an expression of the internal variability of the atmosphere, it may be pushed toward one polarity by external forcings such as stratospheric ozone depletion and greenhouse gases-forced warming (e.g., Arblaster and Meehl 2006).

An increasing poleward moisture flux with increasing temperature has been remarked upon in climate simulations of global warming since the beginning of climate change research (Manabe and Wetherald 1975). Changes in extremes can be thought of as produced by low-frequency variability in the flow field and therefore in the moisture transport. Even if the statistics of this variability remains unchanged while the magnitude of the horizontal transport of vapour increases, the intensity of extremes will increase, as more water is transported by any particular anomalous flow (Held and Soden 2006).

The subtropical anticyclones and the migratory systems associated to the westerly circulation are the dominant factors that define the climate characteristics of the southern extratropics (e.g. Simmonds 2003). An important consequence of the enhanced moisture fluxes and the poleward shift of circulation is that the polar boundaries of the subtropical anticyclones experience particularly strong drying, affecting parts of Australia, South America and Southern Africa. Concerning extratropical cyclones, IPCC AR4 (Christensen et al. 2007 and references therein) gives an overview of likely projected changes: decrease in the total number of extratropical cyclones, poleward shift of storm track and associated precipitation, increased number of intense cyclones and associated strong winds, increased occurrence of high waves.

2.2 Methodology

Our study is based on seven IPCC AR4 models: GFDL-CM2.0, GFDL-CM2.1, INMCM3.0, IPSL-CM4, MIROC3.2-hires, MIROC3.2-medres and MRI-CGCM2.3.2a. These models have the extreme indices reported for the twentieth century climate

(period 1970–1999) and for the twenty-first century climate (SRES A1B, intermediate scenario balanced across all energy sources, Nakicenovic and Swart 2000, period 2070–2099), over both continental and oceanic areas, to the Program for Climate Model Diagnosis and Intercomparison (PCMDI). Some documentation for the models is available at the PCMDI Web site (http://www-pcmdi.llnl.gov/). These models represent the present-day state-of-the-art in global coupled models.

Input data are annual series of geopotential height at 500 hPa (Z500) and selected extreme indices as described in Frich et al. (2002). The SAM is defined here as the leading empirical orthogonal mode (EOF-1) obtained from Z500 anomalies, over a domain south of 42° S. The anomalies are relative to the best straight-line fit linear trend from every single-model input data and are area weighted by the square root of cosine of latitude. We identify years during which a particular phase of the SAM is strong (years in which the principal component, PC-1, is above one standard deviation of its mean value). As when detrending, the standard deviations are also estimated model by model. Note that usually the SAM is evaluated over a larger domain (e.g. south of 20° S in Carril et al. 2005). However, both choices (42° S and 20° S) give similar results as proved by the very high correlation (∼0.99) between corresponding time series of principal components.

For the sake of brevity, we only present results related to some selected extreme indices:

- Total number of days per year with absolute minimum temperature below 0°C (total number of *frost days*, or Fd as named by Frich et al. 2002).
- Percentage of times in the year when minimum temperature is above the 90th percentile of the climatological distribution for that calendar day (*warm nights*, or Tn90 in Frich et al. 2002).
- Maximum number of consecutive dry days (*dry days*, or CDD in Frich et al. 2002).
- Fraction of total precipitation due to events exceeding the 95th percentile of the climatological distribution for wet day amounts (*precip* > 95th, or R95t in Frich et al. 2002).

We consider that selecting these indices is helpful as a basis to examine processes related with generating the geographic patterns of changes in temperature and precipitation extremes in the southern extratropics. In line with recent literature pointing out the weakness associated with statistical tests when the signal being sought is masked by large variability (e.g. Trenberth 2005), in this paper we emphasized the physical understanding and the consistency of the changes in the different extreme indices (and not their statistical significance).

3 Mean patterns of change

The multi-model averages of spatial patterns of late twentieth century climatology and change (2070–2099 minus 1970–1999) for each index are shown in Fig. 1. The total number of frost days (Fd, panels a, b) is an index particularly pertinent to the extratropical regions and it is associated with anomalies in the length of spring and fall seasons (Tebaldi et al. 2006). Consistent with the general warming during the twenty-first century associated with increasing greenhouse gas emissions, models

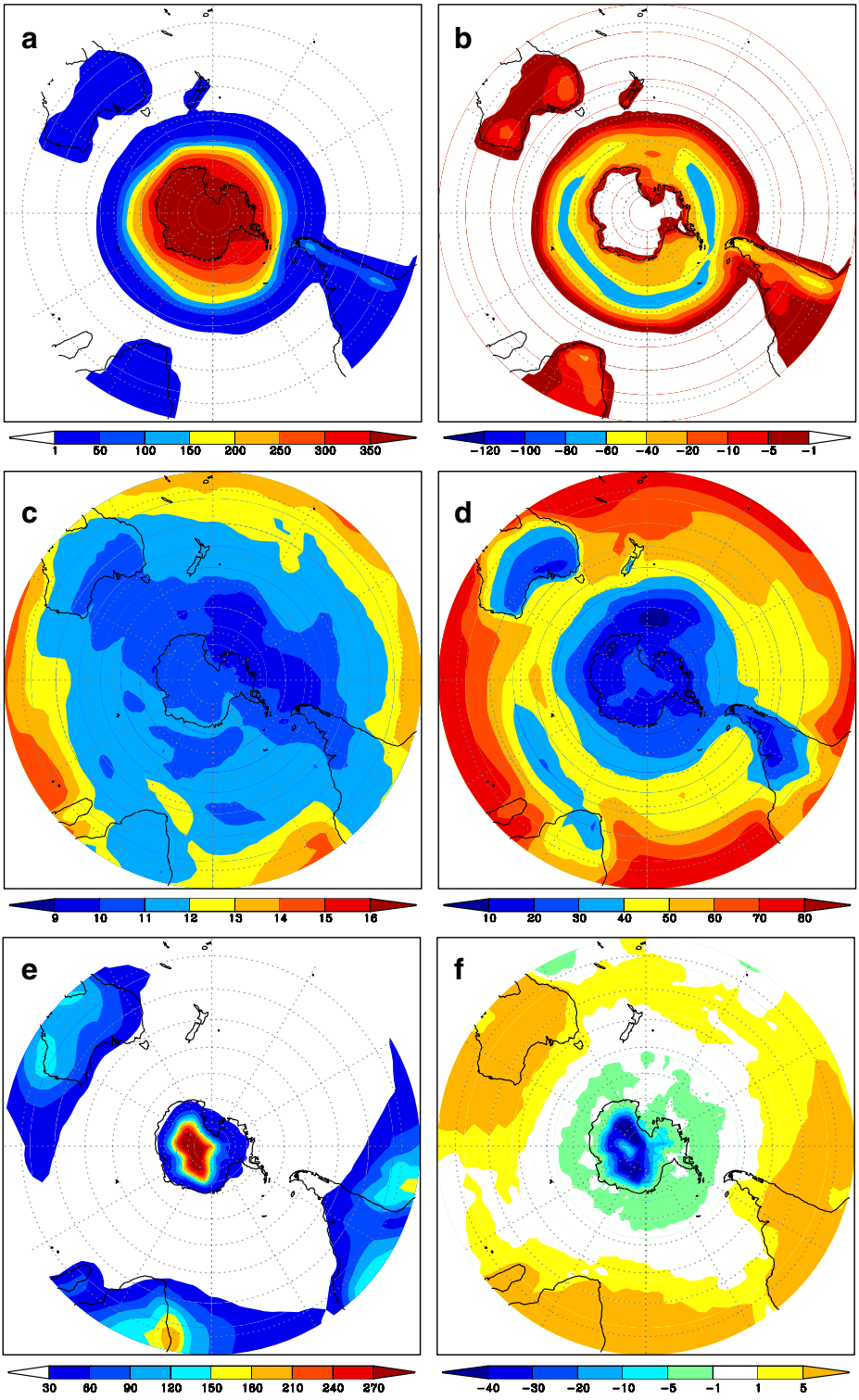
a
1 50 100 150 200 250 300 350
b
−120 −100 −80 −60 −40 −20 −10 −5 −1
c
9 10 11 12 13 14 15 16
d
10 20 30 40 50 60 70 80
e
30 60 90 120 150 180 210 240 270
f
−40 −30 −20 −10 −5 −1 1 5

◀ **Fig. 1** Multi-model averages of spatial patterns of extreme indices for 1970–1999 (*left column*) and change under A1B scenario (2070–2099 minus 1970–1999, *right column*). Temperature extreme indices are Fd (**a**, **b**) and Tn90 (**c**, **d**). Precipitation indices are CDD (**e**, **f**) and R95t (**g**, **h**). See text for description of indices. Units: Fd in days, Tn90 in percent, CDD in days and R95t in percent

project a decrease in cold extremes throughout the southern mid- to high latitudes and in the southern sectors of Africa, Australia and South America. Overall the most significant reductions in Fd are confined to regions where snow and sea ice retreat with global warming. In the Southern Ocean the reduction in the number of frost days is a maximum along the sea ice edge mainly as a result of sea ice melting in winter under global warming. Over the continents, the changes are larger in South America along the Andes Mountains probably related with changes in the 0°C isotherm height.

In general, changes in extreme temperature indices are consistent with less cold minimum temperature extremes (e.g., Fd) and more warm minimum temperature extremes (e.g., Tn90). The present climate pattern of Tn90 (panel c) shows an equator-to-pole negative gradient with particularly low values in the central and eastern southern Pacific. Its change (panel d) decreases poleward and is systematically positive throughout the southern extratropics, being weaker over land masses than over oceans. In southern South America the changes in the frequency of warm nights tend to be less important along the eastern coast, consistent with a larger mean warming along the Andes, especially in summer (see Fig. 11.15 in Christensen et al. 2007). However, the percentage of time in the year with warm nights e.g. in southern La Plata Basin would be more than twice the typical frequency during the late twentieth century climate.

The maximum number of consecutive dry days (CDD; panels e, f) is an index suitable to measure the hypothesized tendency towards longer dry spells separating intensified wet events (Tebaldi et al. 2006). Actually, longer dry spells (positive

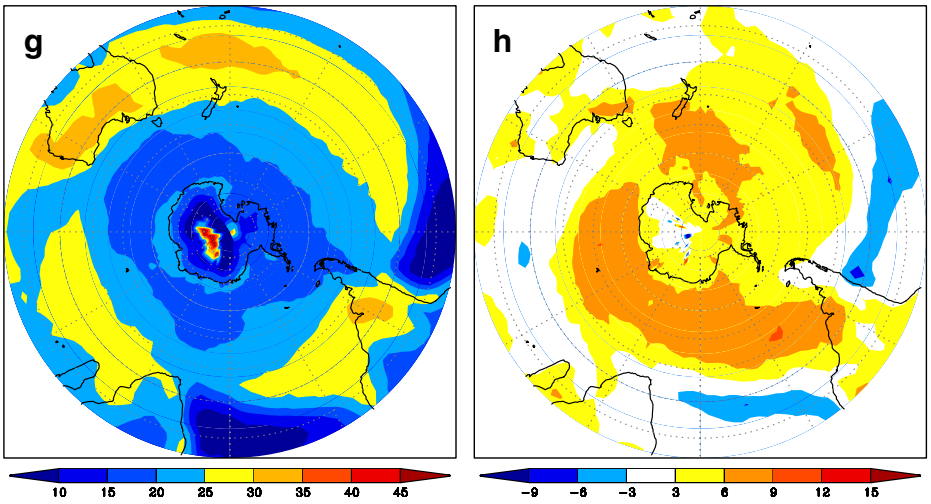

Fig. 1 (continued)

changes in CDD) are expected over most land masses of the SH to the north of 45° S. In contrast, the mid- to high latitudes over the Southern Ocean see a shortening of periods between rainfall events. The index R95t (panels g, h) measures changes in the intensity of precipitation. The future projection of R95t shows a tendency towards larger values of this index over most land masses in the SH, but the largest positive changes in R95t occur over the Southern Ocean. Negative changes take place along 30° S, especially in the regions affected by the eastern South Pacific and South Atlantic subtropical anticyclones. The basic banded structure of changes in both extreme precipitation indices is consistent with the combination of the two aforementioned key processes associated with global warming (enhancement of moisture fluxes and poleward shift of extratropical circulation). These findings are coherent with the results described in Lim and Simmonds (2007) concerning the observed increase in the cyclone density, intensity, and translational velocity and in the number of explosively developing cyclones in the southern extratropics over 1979–2001. Results are also coherent with Lynch et al. (2006) concerning changes in synoptic weather patterns around Antarctica. By using a ten-member multimodel ensemble they show a future change to more cyclonicity and stronger westerlies in the sub Antarctic seas. The increase in cyclonic developments, particularly deep ones, is reflected in precipitation increases. This trend is quite consistent among the models, and is reflected also in an increase in positive SAM index. According to Lynch et al. (2006), the coherence of temperature and precipitation anomaly patterns and their trends reflects the extent to which these are related to circulation.

Of particular interest for CLARIS, note that south eastern South America near the Rio de la Plata, a region with large values of R95t during the present climate time slice, would experience an increase of this index by the end of the twenty-first century. In addition this is a region where mean precipitation is projected to increase across the IPCC AR4 models (Christensen et al. 2007) and where the number of consecutive dry days also tends to increase (i.e. longer periods between rainfall events). As a consequence, rainfall events in the southern La Plata Basin during the twenty-first century would be less frequent but considerably more intense.

Another feature of particular concern for southern South America is the significant reduction in the number of days with minimum temperature below 0°C, a key factor linked to cryospheric processes. In temperate mountain regions, the snowpack is often close to its melting point, so that it may respond rapidly to minor changes in temperature, as has been observed in most glaciers along the Andes (e.g. Rignot et al. 2003). As warming increases in the future, regions where snowfall is the current norm will increasingly experience precipitation in the form of rain (Leung et al. 2004; Christensen et al. 2007). The corresponding changes in mountain hydrology will affect the lowland regions that depend on mountain water resources for domestic, agricultural, energy and industrial supply.

4 Estimating the risk of future severe extreme indices

In what follows we concentrate in the occurrence of the severest phenomena (represented by the years with the highest indices during the present climate) and their future changes. In order to assess the changing probability of the severe extreme indices for the time period 2070 to 2099 we adopt a methodology similar to Räisänen

and Palmer (2001) and Palmer and Räisänen (2002), based on the risk of any dichotomous climate event as determined by an ensemble of climate projections.

Years characterized by the occurrence of severe extreme phenomena are found as follows. Examining all of the years simulated by a particular model in the 1970–1999 time slice, the highest six values (annual indicators) of a particular extreme index during these 30 years can be deemed as an estimate of the index of the most extreme 20% of all years in the current climate. For example, Fig. 2a represents the corresponding 80% percentile of the probability density function of the index R95t for the twentieth century time slice. Using the terminology of Palmer and Räisänen

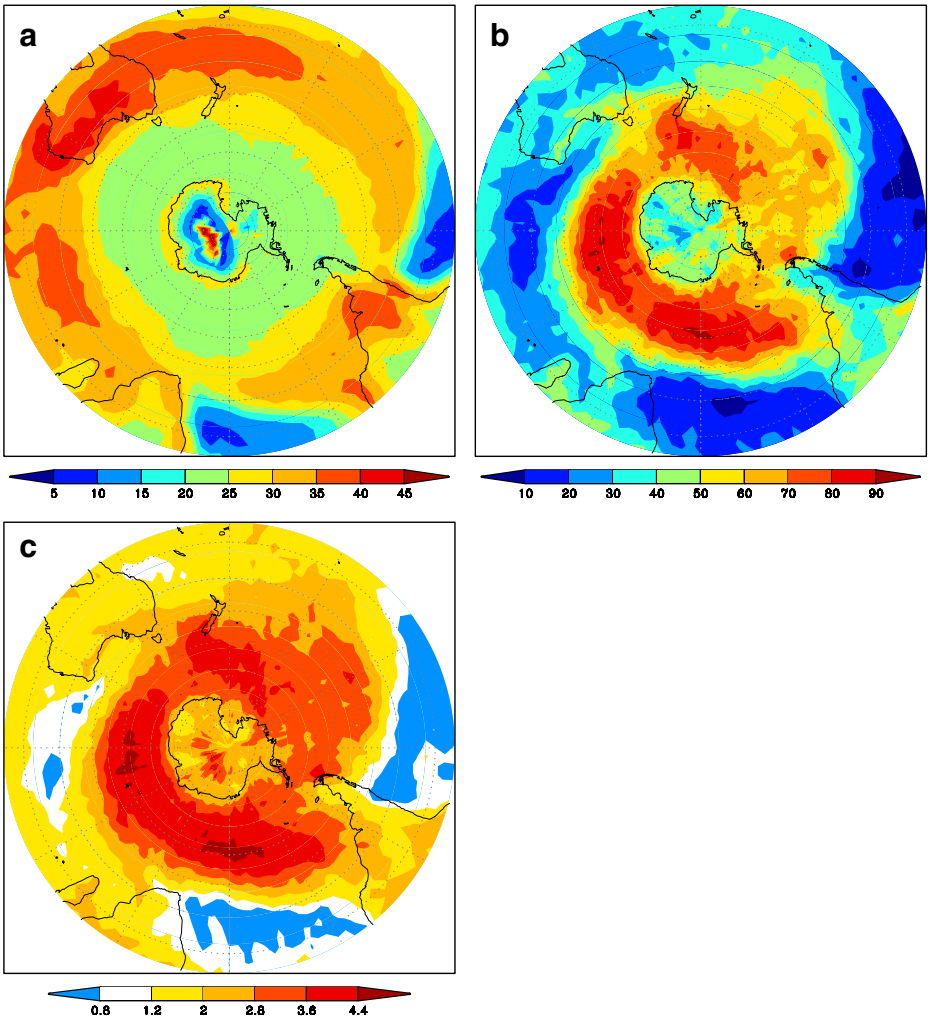

Fig. 2 **a** Eighty percent percentile of the probability density function of R95t for 1970–1999 given the "score" of a "severe" year (in units of R95t, i.e. percent). **b** Fraction (%) of years during 2070–2099 exceeding the score (given in **a**). **c** The ratio of values in **b** divided by 20%, given the change in risk of a "severe" year (non-dimensional unit)

(2002), we consider the dichotomous event E, defined to occur if the index R95t at a specific location exceeds this "score" associated with twentieth century levels of greenhouse gases. The likelihood of having a year with values of R95t at a specific location larger than the score value is 20%. This gives a baseline for assessing future changes in this index (i.e. the baseline twentieth century probability of E is 20%, corresponding to an expected return period of 5 years).

The future climate time slice (2070–2099) is then examined, and the fraction of years exceeding the score (defined by Fig. 2a) determined. This is referred to as the likelihood of particularly extreme years relative to the considered index. We compare each model's future with its own present climate to help avoid distortions due to potential disagreeing biases in the different models. The results are shown in Fig. 2b after averaging over models. Values smaller (larger) than 20% indicate a decrease (increase) in the frequency of years characterized by particularly intense extremes. By the end of twenty-first century, the likelihood of such extreme precipitation intensity is projected to rise in most areas with the exception of the subtropical anticyclones, which (as discussed above) experience particularly strong drying. Over the Southern Ocean the likelihood has increased to over 60% (i.e. at least 18 out of 30 years would experience severe values of R95t during the period 2070–2099), consistent with the increased number of intense cyclones and with the poleward shift of the storm tracks.

In Fig. 2c we show the ratio of the likelihoods in both periods (i.e. values in Fig. 2b divided by 20%) giving a measure of the changing risk of the event E resulting from anthropogenic forcing. For example, in southern South America the likelihood of occurrence of years with severe values of R95t in the Rio de la Plata region is estimated to increase by a factor of about 2.5 during 2070–2099. On the contrary, over central Chile this likelihood would decrease by a factor of about 0.8. Note that this pattern of enhanced precipitation extremes in south eastern South America and less precipitation extremes over parts of southern Andes, is similar to the regional pattern of mean precipitation changes discussed in the IPCC AR4 (Christensen et al. 2007).

Figure 3 shows the ratio of likelihoods (as in Fig. 2c) but for the other three indices (Fd, Tn90 and CDD). Concerning temperature indices, the most significant feature occurs to the north of the Ross Sea. In the second time slice, years with large values of Fd (Fig. 3a) virtually vanish all over the hemisphere (ratios $\sim$0) with the main exception of the region to the south of New Zealand, where the likelihood of having a year with a large number of frost days would decrease by a factor in the range 0.1 to 0.9. The Weddell Sea has a similar behavior but with smaller ratios. Concerning Tn90 (Fig. 3b), the significant increase in the annual occurrence of warm minimum temperatures increases the likelihood of having years with severe values of that index during 2070–2099 (as defined above, "severe" values are those values exceeding the 80% percentile of the period 1970–1999). Throughout the whole SH, with the exception of some oceanic areas around Antarctica, the likelihood of occurrence of these kinds of years is estimated to increase by a factor of (at least) 4 by the end of this century. The increase in the number of years with a large number of days with very warm minimum temperatures tends to be smaller to the north of the Ross Sea (ratios in the range 1 to 3). Corresponding estimates of the changing probability of E for CDD (Fig. 3c) show a banded structure with increased likelihood of severe dry spells to the north of about 50° S and decreased likelihood in the sub Antarctic seas.

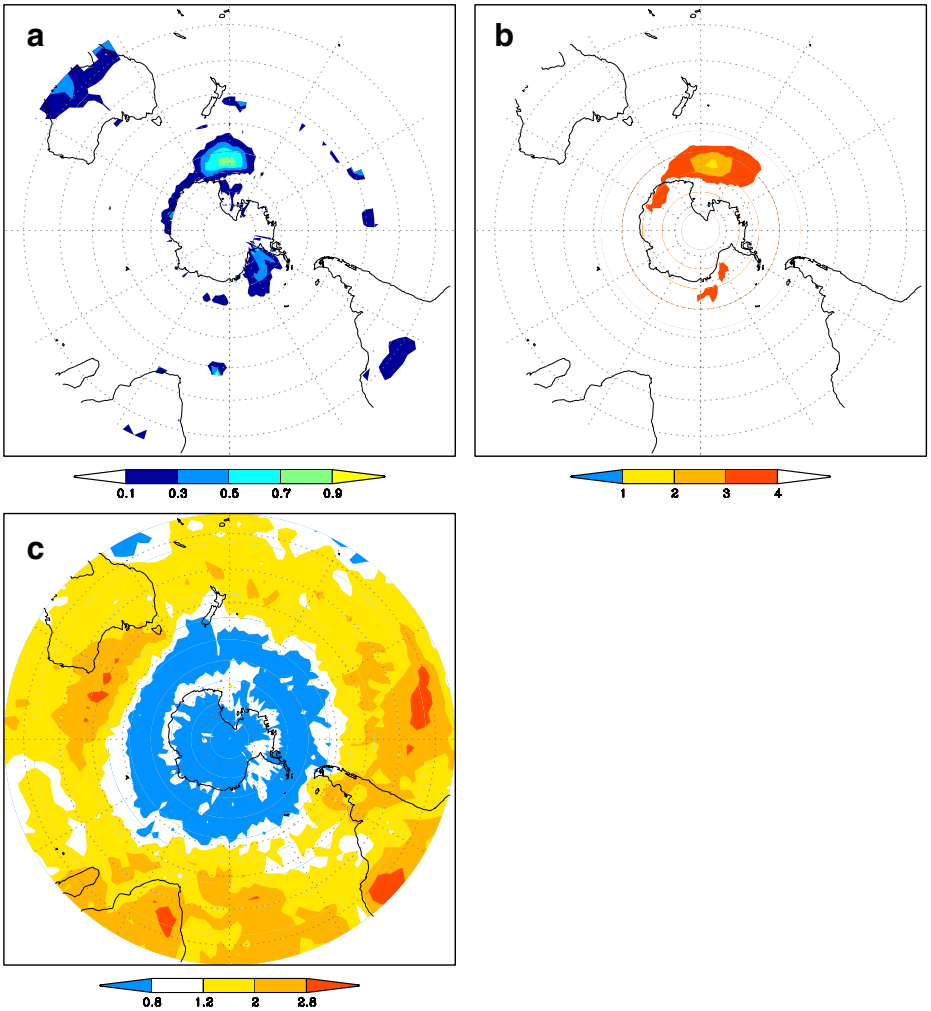

Fig. 3 Ratio of likelihoods (as in Fig. 2c) but for **a** Fd, **b** Tn90 and **c** CDD. Non-dimensional units

Note that over parts of Brazil and South Africa the risk of having very long dry spells would increase by a factor of 3. In southern South America this risk about doubled between both time slices.

5 Relationship between severe extreme indices and SAM

Changes in circulation would contribute to the pattern of extreme changes at middle and high latitudes (Meehl et al. 2005). In order to explore the circulation changes associated with the SAM, we evaluate the EOF-1 of annual mean Z500 anomalies for both time slices. Figure 4 shows the results for the first period and the difference (2070–2099 minus 1970–1999). In the present day time slice (left panel), the positive

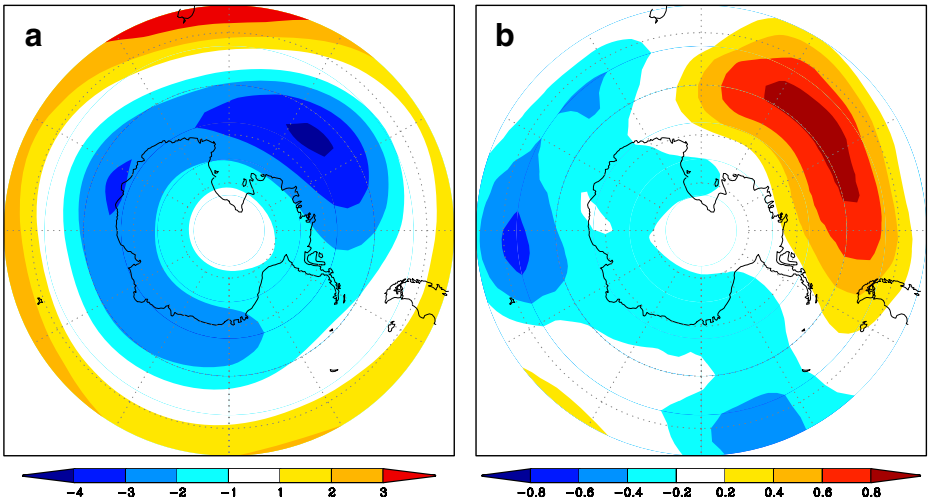

Fig. 4 First EOF of annual mean Z500 anomalies for 1970–1999 (*left panel*) and the difference (2070–2099 minus 1970–1999, *right panel*). Non-dimensional units

phase of the SAM is accompanied by large heat and humidity advections over the Antarctic Peninsula sector. The spatial pattern of the EOF-1 in the second time slice (not shown) is more zonally symmetric and the loadings derived from the A1B scenario are weaker in the south eastern Pacific compared to the present climate (right panel). Consequently, the poleward advection over the Antarctic Peninsula associated with the SAM positive phase tends to weaken during the late twenty-first century. In contrast, it tends to increase near the Ross Sea.

So as to explore the possible influence of the SAM on the risk of severe values of extremes indices, we count the number of years during 2070–2099 in which a particular index exceeds the corresponding score (80% percentile of the period 1970–1999) and during which the positive or negative phases of the SAM are strong (annual PC-1 above one standard deviation of its mean value). As above, we compare each model's future with its own present climate and then we average over models.

Figure 5 shows the number of years in the period 2070–2099 with severe values of Tn90 and during which the phase of SAM is strongly positive (panel a) or negative (panel b). The difference between both panels (Fig. 5c) suggests that the positive phase inhibits the extremely warm minimum temperatures in the Southern Ocean, with the exception of the eastern Bellingshausen Sea. The largest differences are found to the north of the Ross Sea. Over the continents and oceans to the north of about 50° S, this index shows almost no change in the positive phase compared to the negative phase. The influence of SAM on the temperature extremes is not annular and, indeed, it is reminiscent of the dipole sea ice variations described e.g. in Lefebvre and Goosse (2005) with anomalies of opposite sign in the Ross Sea and Antarctic Peninsula-Weddell Sea sectors. This pattern appears driven by a decrease in sea level pressure in the Amundsen-Bellingshausen Sea when SAM is in its positive phase. This induces a deflection of the westerlies towards the south-east around the Peninsula and towards the north-east in the Ross sector. These winds advect warmer air in the Weddell Sea and colder air in the Ross Sea, and alter also the wind-driven

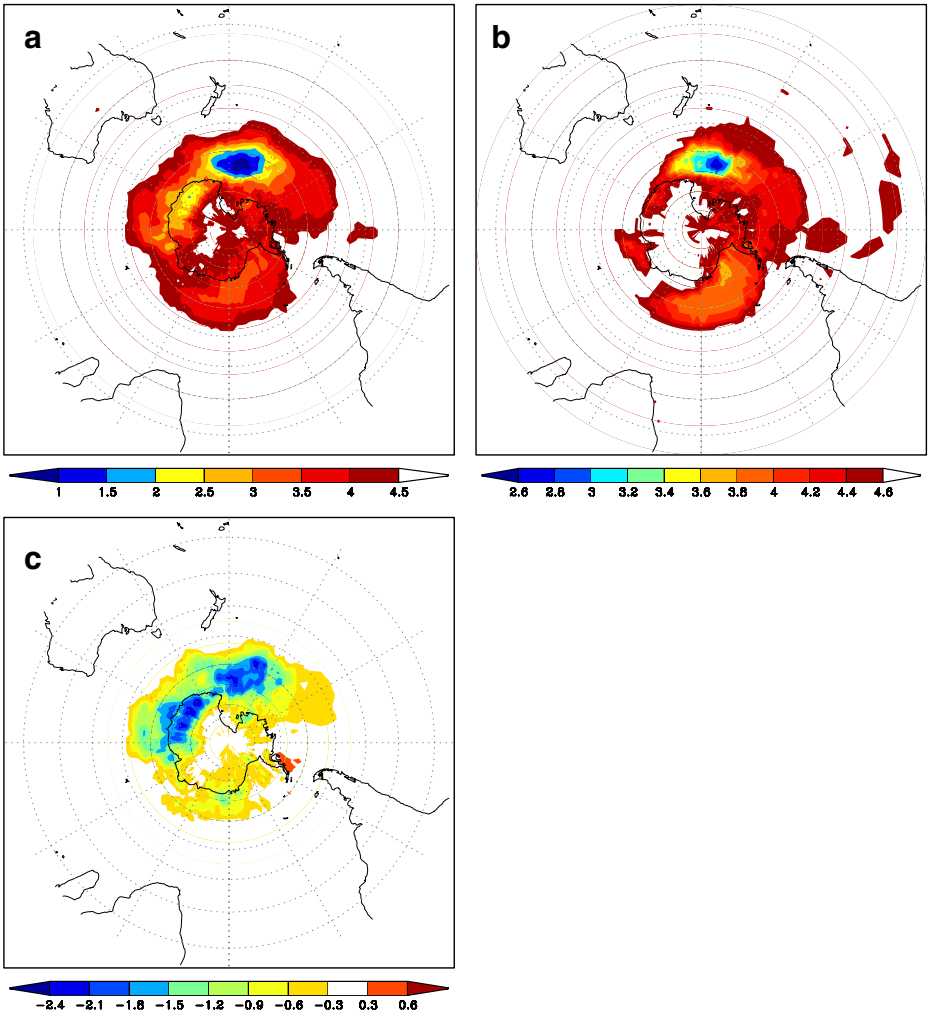

Fig. 5 **a** Number of years during 2070–2099 with "severe" values of Tn90 and with SAM in strong positive phase. **b** As **a** but SAM in strong negative phase. **c** Difference between both *panels* (positive SAM minus negative SAM). Units: years

sea ice export and the advection of heat by the ocean current, resulting in a dipole-like pattern of anomalies (Lefebvre et al. 2004). These findings are consistent with the results for Fd (not shown), suggesting that positive SAM induces severe frost days to the north of the Ross Sea (see also Menéndez and Carril 2006).

Sea ice plays a complex role in the changes in the high southern latitudes (e.g. Lefebvre and Goosse 2007; Stammerjohn et al. 2008). A related question is how well the AR4 models simulate Antarctic sea ice. According to Carril et al. (2005) the sea-ice concentration ensemble-mean values are in rough accord with observational datasets. Models tend on average to produce too little sea ice cover (except along sectors of the sea-ice edge region where the sea-ice extent is slightly overestimated)

and to amplify the amplitude of its seasonal cycle. But the large interannual variability and the large across-model scatter (especially in the Weddell Sea) make the comparison with observations difficult. The relatively good performance of the ensemble-mean results from the averaging of some models with too small sea ice cover and others with too large sea ice cover (Arzel et al. 2006).

Maximum westerlies shift southward during positive SAM and to the north in negative SAM. The low-level atmosphere over the sub-Antarctic seas becomes more convergent during the positive SAM, leading to an increase in rising motion within the air column, which would induce greater precipitation (Gordon et al. 2005). During negative SAM the opposite condition prevails, that of reduced rising motion and drier conditions. In essence, in the negative polarity the drier Antarctic high pressure conditions extend over the adjacent seas. Consistently, severe dry spells are inhibited during the positive phase (Fig. 6a), possibly associated with poleward migration of cyclonic eddies and increasing poleward moisture flux. The mid-latitudes, including most of Patagonia, show the opposite behaviour. Interestingly, the influence of SAM on CDD presents qualitatively similar characteristics at all longitudes.

Figure 6b shows the differences in the number of years with severe values of R95t for years when the SAM is in the high-versus-low index polarities. Positive (negative) values indicate an increased (decreased) likelihood of significant precipitation events when the SAM is in strong positive phase. For example, we note an increase in the likelihood of significant rainfall events in southeast Australia and a decrease in southern Patagonia during the high index polarity. This pattern for Australia is broadly consistent with that observed over the period 1979–2005 (Hendon et al. 2007). The Southern Ocean reveals, in general, a non-uniform, patchy distribution with both increases and decreases in the intensity of heavier precipitation during positive SAM. However, the pattern of zonal mean changes (Fig. 7) show negative differences throughout the mid- to high southern latitudes. In the positive polarity the polar cell of mean meridional circulation anomalies associated with the SAM

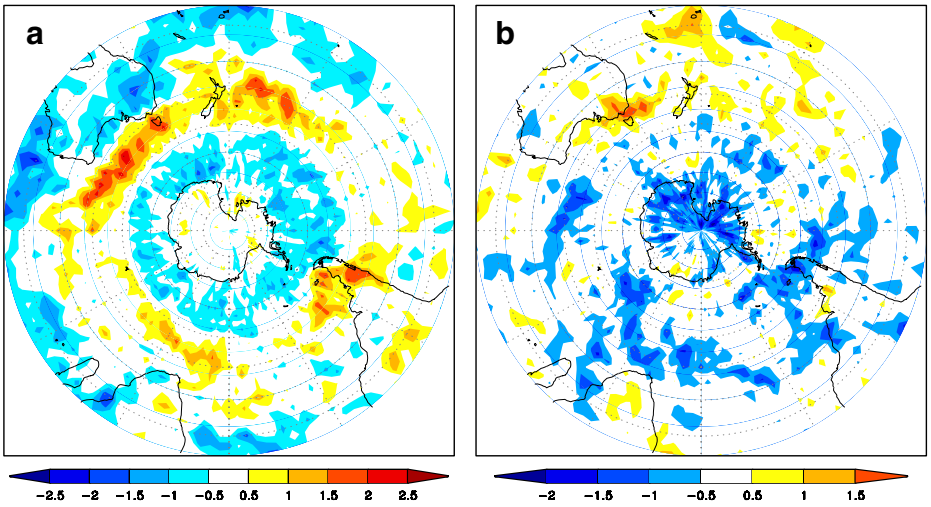

Fig. 6 As Fig. 5c but for **a** CDD and **b** R95t. Units: years

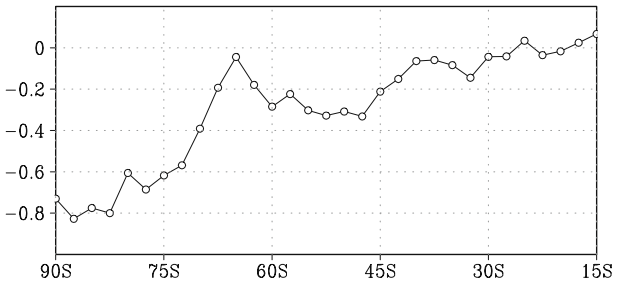

Fig. 7 Zonal mean change from strong positive SAM to strong negative SAM during 2070–2099 in the number of years with "severe" R95t (i.e., as Fig. 6b, but zonally averaged)

is characterized by anomalous rising motion over subpolar latitudes and subsidence over the mid-latitudes (Thompson and Wallace 2000). This is consistent with the tendency towards less values of R95t along most of the mid latitude oceans. The pattern is more difficult to interpret in the higher latitudes where the atmosphere is more convergent, with increasing rising motion in positive SAM. According to Solman and Menéndez (2002), as synoptic systems develop over regions of strong low-level baroclinicity and strong winds (as the sub Antarctic seas during positive SAM) their life cycle is more explosive and they do not grow enough to radiate energy upward. As a consequence, they do not reach a robust development with extremely strong upward motions (as required for extreme precipitation events, Emori and Brown 2005; see also Lim and Simmonds 2002, for a discussion on explosive cyclone development in the Southern Ocean).

6 Final remarks

We have documented the response of four extreme annual indicators (number of frost days, percentage of days with warm minimum temperature, maximum number of consecutive dry days, and fraction of total precipitation due to intense events) as simulated by state of the art coupled models. A subset of the IPCC AR4 multi-model ensemble was treated as a probabilistic climate change projection. The likelihoods for significant anomalous years in terms of available extreme indices related to climate change (e.g., that a given extreme index by the end of the twenty-first century will exceed the most severe 20% of all years during the period 1970–1999) were inferred by counting the number of years in which the event occurs for each particular model. According to Palmer and Räisänen (2002) such probabilistic projections have greater potential value than deterministic projections from either single integrations or from a classical "consensus" approach. On the other hand, the benefit of using a multi-model ensemble (over a single-model ensemble) accrues from sampling some of the inevitable uncertainties in climate simulation. However, two caveats should be mentioned: the ensemble does not necessarily span all models uncertainties and is based on a single idealized anthropogenic forcing scenario (A1B).

The likelihood of severe precipitation intensity has increased to over 60% over the Southern Ocean. On the contrary, subtropical anticyclones experience particularly strong drying. Corresponding estimates of the changing likelihood for very long dry spells show a banded structure with positive ratios to the north of about 50° S and negative ratios in the sub Antarctic seas. In southern South America this risk about

doubled between 1970–1999 and 2070–2099. The changes in precipitation indices are associated with the large increases of temperature and moisture-holding capacity of the air and with the poleward shift of the storm track.

Another concern of this research has relied on the influence of the SAM on extreme indices in the annual time-scale, as this is a critically important aspect for understanding climate trends and projections in the southern extratropics. The SAM could shape not only the mean conditions, but also the daily variability. Consequently extreme events could be sensitive to SAM-related changes in the characteristics of extratropical storms, blocking highs and cold air outbreaks. Its positive phase inhibits the extremely warm minimum temperatures in the Southern Ocean, with the exception of the eastern Bellingshausen Sea, and favors severe frost days to the north of the Ross Sea. Severe dry spells are inhibited during the positive phase along the sub Antarctic seas, while the mid-latitudes, including most of Patagonia, show the opposite behaviour. Our results suggest that the southern continental land masses will experience little significant impact from the SAM during 2070–2099, with some exceptions (e.g. Patagonia and southern Australia for precipitation indices). This is in part justified because much of the inhabitable landmasses are northward of the region where the SAM produces its largest changes in circulation. A caveat needs to be considered regarding the SAM influence on temperature extremes as we did not consider maximum temperature extremes in this study. A recent paper by Kenyon and Hegerl (2008) showed that maximum and minimum temperature extremes may be affected differently during positive and negative phases of large scale circulation modes. Therefore, an interesting question for future research would be whether the SAM influences maximum and minimum temperatures differently in the southern mid- to high latitudes.

As the final word, we caution that our assessment regarding changes in extremes under global warming should be considered as qualitative considering the large range of uncertainty in the factors driving climate change and in its simulation. Moreover, this kind of extreme risk analysis would benefit from an increase in the resolution of climate models and from larger ensembles.

Acknowledgements This research was done in the framework of CLARIS EU project. Comments by two anonymous reviewers helped to improve the manuscript. We acknowledge the international modeling groups for providing their data for analysis, the Program for Climate Model Diagnosis and Intercomparison (PCMDI) for collecting and archiving the model data, the JSC/CLIVAR Working Group on Coupled Modelling (WGCM) and their Coupled Model Intercomparison Project (CMIP) and Climate Simulation Panel for organizing the model data analysis activity, and the IPCC WG1 TSU for technical support. The IPCC Data Archive at Lawrence Livermore National Laboratory is supported by the Office of Science, US Department of Energy. C.G. Menéndez was partially supported by project PIP 5416 (CONICET, Argentina).

References

Alexander LV, Arblaster JM (2008) Assessing trends in observed and modelled climate extremes over Australia in relation to future projections. Int J Climatol 29:417–435. doi:10.1002/joc.1730

Arblaster JM, Meehl GA (2006) Contributions of external forcings to southern annular mode trends. J Clim 19:2896–2905

Arzel O, Fichefet T, Goosse H (2006) Sea ice evolution over the 20th and 21st centuries as simulated by current AOGCMs. Ocean Model 12:401–415

Cai W, Whetton PH, Karoly DJ (2003) The response of the Antarctic oscillation to increasing and stabilized atmospheric CO_2. J Clim 16:1525–1538
Carril AF, Navarra A (2001) The interannual leading modes of the extratropical variability in the southern hemisphere simulated by the ECHAM-4 atmospheric model. Clim Dyn 18:1–16
Carril AF, Menéndez CG, Navarra A (2005) Climate response associated with the southern annular mode in the surroundings of Antarctic Peninsula: a multimodel ensemble analysis. Geophys Res Lett 32:L16713. doi:10.1029/2005GL023581
Chapman WL, Walsh JE (2006) A synthesis of Antarctic temperatures. J Clim 26:1181–2119
Christensen JH, Hewitson B, Busuioc A, Chen A, Gao X, Held I, Jones R, Kolli RK, Kwon W-T, Laprise R, Rueda VM, Mearns L, Menéndez CG, Räisänen J, Rinke A, Sarr A, Whetton P (2007) Regional climate projections. In: Solomon S, Qin D, Manning M, Chen Z, Marquis M, Averyt KB, Tignor M, Miller HL (eds) Climate change 2007: the physical science basis. Contribution of working group I to the fourth assessment report of the intergovernmental panel on climate change. Cambridge University Press, Cambridge
Christidis N, Stott PA, Brown S, Hegerl G, Caesar J (2005) Detection of changes in temperature extremes during the second half of the 20th century. Geophys Res Lett 32:L20716. doi:10.1029/2005GL023885
Emori S, Brown SJ (2005) Dynamic and thermodynamic changes in mean and extreme precipitation under changed climate. Geophys Res Lett 32:L17706. doi:10.1029/2005GL023272
Frich P, Alexander LV, Della-Marta P, Gleason B, Haylock M, Klein Tank AMG, Peterson T (2002) Observed coherent changes in climatic extremes during the second half of the twentieth century. Clim Res 19:193–212
Gordon AL, Visbeck M, Comiso JC (2005) Did a prolonged negative SAM produce the Weddell Polynya of the 1970s? CLIVAR Exchanges 35:17–20
Haylock MR et al (2006) Trends in total and extreme South American rainfall in 1960–2000 and links with sea surface temperature. J Clim 19:1490–1512
Hegerl GC, Zwiers FW, Braconnot P, Gillett NP, Luo Y, Marengo Orsini JA, Nicholls N, Penner JE, Stott PA (2007) Understanding and attributing climate change. In: Solomon S, Qin D, Manning M, Chen Z, Marquis M, Averyt KB, Tignor M, Miller HL (eds) Climate change 2007: the physical science basis. Contribution of working group I to the fourth assessment report of the intergovernmental panel on climate change. Cambridge University Press, Cambridge
Held IM, Soden BJ (2006) Robust responses of the hydrological cycle to global warming. J Clim 19:5686–5699
Hendon HH, Thompson DWJ, Wheeler MC (2007) Australian rainfall and surface temperature variations associated with the southern hemisphere annular mode. J Clim 20:2452–2467
Kenyon J, Hegerl GC (2008) Influence of modes of climate variability on global temperature extremes. J Clim 21:3872
Kharin VV, Zwiers FW, Zhang X, Hegerl GC (2007) Changes in temperature and precipitation extremes in the IPCC ensemble of global coupled model simulations. J Clim 20:1419–1444
Kiktev D, Sexton D, Alexander L, Folland C (2003) Comparison of modelled and observed trends in indicators of daily climate extremes. J Clim 16:3560–3571
Kiktev D, Caesar J, Alexander LV, Shiogama H, Collier M (2007) Comparison of observed and modeled trends in annual extremes of temperature and precipitation using the results of several climate models. Geophys Res Lett 34:L10702. doi:10.1029/2007GL029539
Kushner PJ, Held IM, Delworth TL (2001) Southern hemisphere atmospheric circulation response to global warming. J Clim 14:2238–2249
Lefebvre W, Goosse H (2005) Influence of the southern annular mode on the sea ice-ocean system: the role of the thermal and mechanical forcing. Ocean Sci Discuss 2:299–329
Lefebvre W, Goosse H (2007) Analysis of the projected regional sea-ice changes in the southern ocean during the twenty-first century. Clim Dyn 30:59–76
Lefebvre W, Goosse H, Timmermann R, Fichefet T (2004) Influence of the southern annular mode on the sea ice-ocean system. J Geophys Res 109:C09005. doi:10.1029/2004JC002403
Leung LR, Qian Y, Bian X, Washington WM, Han J, Roads JO (2004) Mid-century ensemble regional climate change scenarios for the western United States. Clim Change 62:75–113
Lim E-P, Simmonds I (2002) Explosive cyclone development in the southern hemisphere and a comparison with northern hemisphere events. Mon Weather Rev 130:2188–2209
Lim E-P, Simmonds I (2007) Southern Hemisphere winter extratropical cyclone characteristics and vertical organization observed with the ERA-40 reanalysis data in 1979–2001. J Clim 20:2675–2690

Lynch A, Uotila P, Cassano JJ (2006) Changes in synoptic weather patterns in the polar regions in the 20th and 21st centuries, part 2: Antarctic. Int J Climatol 26:1181–2119
Manabe S, Wetherald RT (1975) The effect of doubling CO_2 concentration on the climate of the general circulation model. J Atmos Sci 32:3–15
Meehl GA, Arblaster JM, Tebaldi C (2005) Understanding future patterns of increased precipitation intensity in climate model simulations. Geophys Res Lett 32:L18719. doi:10.1029/2005GL023680
Meehl GA, Arblaster JM, Tebaldi C (2007) Contributions of natural and anthropogenic forcing to changes in temperature extremes over the United States. Geophys Res Lett 34:L19709. doi:10.1029/2007GL030948
Meneghini B, Simmonds I, Smith IN (2007) Association between Australian rainfall and the southern annular mode. Int J Climatol 27:109–121
Menéndez CG, Carril AF (2005) SAM-related variations in the Antarctic Peninsula from IPCC AR4 models. CLIVAR Exchanges 35:7–9
Menéndez CG, Carril AF (2006) On the relationship between SAM and frost days as represented by an ensemble of IPCC AR4 models. CLARIS News 5:21–25
Nakicenovic N, Swart R (eds) (2000) Special report on emissions scenarios: a special report of working group III of the intergovernmental panel on climate change. Cambridge University Press, Cambridge, 599 pp
Palmer TN, Räisänen J (2002) Quantifying the risk of extreme seasonal precipitation events in a changing climate. Nature 415:512–514
Pezza AB, Simmonds I, Renwick JA (2007) Southern hemisphere cyclones and anticyclones: recent trends and links with decadal variability in the Pacific Ocean. Int J Climatol 27:1403–1419
Räisänen J, Palmer TN (2001) A probability and decision-model analysis of a multi-model ensemble of climate change simulations. J Clim 14:3212–3226
Randall DA, Wood RA, Bony S, Colman R, Fichefet T, Fyfe J, Kattsov V, Pitman A, Shukla J, Srinivasan J, Stouffer RJ, Sumi A, Taylor KE (2007) Climate models and their evaluation. In: Solomon S, Qin D, Manning M, Chen Z, Marquis M, Averyt KB, Tignor M, Miller HL (eds) Climate change 2007: the physical science basis. Contribution of working group I to the fourth assessment report of the intergovernmental panel on climate change. Cambridge University Press, Cambridge
Raphael MN, Holland MM (2006) Twentieth century simulation of the southern hemisphere climate in coupled models. Part 1: large scale circulation variability. Clim Dyn 26:217–228
Rauthe M, Hense A, Paeth H (2004) A model intercomparison study of climate change signals in extratropical circulation. Int J Climatol 24:643–662
Reason CJC, Rouault M (2005) Links between Antarctic oscillation and winter rainfall over western South Africa. Geophys Res Lett 32:L07705
Rignot E, Rivera A, Casassa G (2003) Contribution of the Patagonia Icefields of South America to sea level rise. Science 302:434–437
Rusticucci M, Marengo J, Penalba O, Renom M (2006) Comparisons between observed and modeled precipitation and temperature extremes in South America during the XX century (IPCC 20C3M). In: Proceedings of 8 ICSHMO, Foz do Iguaçu, Brazil, 24–28 April 2006, INPE, pp 379–389
Rusticucci M, Marengo J, Penalba O, Renom M (2009) An intercomparison of modelsimulated in extreme rainfall and temperature events during the last half of the XX century: part 1: mean values and variability. Clim Change (this issue)
Schneider DP, Steig EJ, Comiso JC (2004) Recent climate variability in Antarctica from satellite-derived temperature data. J Clim 17:1569–1583
Sillmann J, Roekner E (2008) Indices for extreme events in projections of anthropogenic climate change. Clim Change 86:83–104
Silvestri GE, Vera CS (2003) Antarctic oscillation signal on precipitation anomalies over southeastern South America. Geophys Res Lett 30:2115
Simmonds I (2003) Modes of atmospheric variability over the Southern Ocean. J Geophys Res 108(C4):8078. doi:10.1029/2000JC000542
Solman SA, Menéndez CG (2002) ENSO-related variability of the Southern hemisphere winter storm track over the eastern Pacific–Atlantic sector. J Atmos Sci 59:2128–2140
Stammerjohn SE, Martinson DG, Smith RC, Yuan X, Rind D (2008) Trends in Antarctic annual sea ice retreat and advance and their relation to El Nino–southern oscillation and southern annular mode variability. J Geophys Res 113:C03S90. doi:10.1029/2007JC004269

Tebaldi C, Hayhoe K, Arblaster JM, Meehl GE (2006) Going to the extremes: an intercomparison of model-simulated historical and future changes in extreme events. Clim Change 79:185–211
Thompson DWJ, Wallace JM (2000) Annular modes in the extratropical circulation. Part I: month-to-month variability. J Clim 13:1000–1016
Trenberth K (2005) Uncertainty in hurricanes and global warming. Science 308:1753–1754
Yin JH (2005) A consistent poleward shift of the storm tracks in simulations of 21st century climate. Geophys Res Lett 32:L18701. doi:10.1029/2005GL023684